

Application of PSE Analysis Method with Transitional Turbulence Model to Typical Hypersonic Flows

Yan Peigang, Qian Xiaoru, Han Wanjin

Abstract—An advanced transitional turbulence model ($\gamma - \text{Re}_\theta$) has been applied to the simulation of the typical hypersonic flows in the present investigation, which is corrected with empirical correlation for the transition consideration. Combining PSE (stability analysis equation) with eN prediction method, it has been studied how to find out the position of the most unstable flow within the boundary layer, so that the transition empirical correlation parameters would be more appropriate for the specified flow while being independent of designer's experiences. The typical hypersonic flow field over a blunt cone has been simulated, through which it could be found that both the computational results of the wall heat flux and boundary layer transition region agree well with the experimental results. Besides t, both the interaction between shock wave with the boundary layer on a flat plat, and the flow across a compression corner have been simulated by the same model as well. It was found that the present methods are also applicable for the simulation of complicated flow with shock wave/boundary layer interaction, and the results turned out to be superior to those employing traditional turbulence models.

Index Terms— Hypersonic flow, PSE Stability Equation, Transition, Shock wave, Boundary layer

I. INTRODUCTION

Turbulence flow is an important phenomenon in fluid dynamics. In the aerodynamic design one of the most difficulties is to simulate the complex turbulence flow. Direct numerical simulation (DNS) of turbulence and Large Eddy Simulation (LES) have good theoretical basis and broad application values. However, limited by the current state-of-the-art calculation conditions, they are not applicable to engineering modeling yet. Though DNS is the most accurate and appropriate method for transition and turbulence study, it still strongly constrained by computer resources and algorithmic limitations. Most current DNS studies are only conducted for very simple geometries. Therefore, using the current turbulence models to solve engineering turbulence problems is still the most effective and most practical choice. Hypersonic flows involve complex flow phenomena, such as large adverse pressure gradient, flow separation and

re-attached as well as the strong effect of compressibility. In the flow transition region, aircraft's surface heat flow rate and the surface friction coefficient will increase dramatically. Therefore, to accurately predict the location of the transition starting point and the length of transition zone is engineering is the key point of engineering design, especially in the thermal protection system design. When calculated by turbulence model, it is obviously unreasonable if the transition location is directly given by empirical formula[1,2]. It is generally believed that the transition and instability mechanism of three-dimensional hypersonic flow have three ways: second-mode, cross-flow and bypass[3]. In order to study these mechanisms, researchers have been

carried out a great deal of research work. The $\gamma - \text{Re}_\theta$ model proposed by Langtry and Menter[4,5] overcomes this difficulty by predicting transition only by the use of local quantities. Martine had attempted to investigate a well-suited hypersonic intake using innovative $\gamma - \text{Re}_\theta$ model in combination with the in-house correlations for transition onset and length. The new model has a great improvement than those used before but it still needs to determine the Reynolds Number of transition starting point by empirical correlation and increase the uncertainty of the numerical calculation^[6].

Stability analysis is one means of studying the physics of the transition problem, such as the LST and PSE methods^[6]. The most popular theoretical prediction method in practical use is to calculate the development of disturbances, and give transition position to reveal the mechanism of it, which is based on linear stability theory of the e^N prediction method. For example, a Hypersonic Boundary Layer package has been developed for the stability and transition analysis^[7-10]. It generates a prediction for the evolution of an initial disturbance when marching downstream from starting point to predict the onset of transition, an experimental correlation is required through the semi-empirical e^N model. However, its limitations is so large that it could not be completely used in the engineering designs^[11,12]. It is not so clear about these mechanisms because of the complexity of the hypersonic flow. The numerical results and experimental ones show a large deviation.

The paper presents an approach to joint these two methods. The specific way is to use e^N method to estimate boundary layer instability location, to calculate the momentum thickness Reynolds number of the transition starting point, to amend transition model empirical relations according to the

Pei-gang Yan, School of Energy Science and Engineering, Harbin Institute of Technology, Harbin, 150001, China, 0

Xiao-ru Qian, School of Energy Science and Engineering, Harbin Institute of Technology, Harbin, 150001, China

Wan-jin Han, School of Energy Science and Engineering, Harbin Institute of Technology, Harbin, 150001, China

situation, to provide the experience factors that could be directly used to flow field calculation and to reduce reliance on the designer experience. The results show that this method can more accurately simulate the transition process and the shock wave/boundary layer interaction caused by separated flow. The wall pressure and heat flux of the transition zone and separation zone are in good agreement with the experiment, which gives a more accurate simulation of supersonic or hypersonic flow of the complex multi-wave system, transitional flows, and aerodynamic heating and so on.

II. $\gamma - Re_\theta$ TRANSITION MODEL

To accurately solve hypersonic flows, the time-averaged Navier Stokes equations are solved by spatial discretization. Fluent software is adopted as the numerical solver. MUSCL scheme with third-order accuracy and implicit time-advance scheme are also used.

The flow field changes severely in the shock wave/boundary layer interaction region, where the turbulence is unbalanced, especially under the interaction of strong shock wave. However, turbulence model treats the turbulent fluctuation statistics and the averaged quantities separately, and uses the averaged quantities to model the pulse statistics[13]. The general Turbulence models are not enough to accurately reflect the characteristics of the non-equilibrium, that is said, have no adequate abilities to describe the dependence of the pulse statistics quantities on the averaged in the process from the non-equilibrium to the balance. Thus the physical characteristics of turbulence pressure enhanced after the shock wave as well as the heat flow are all overestimated[14]. In this paper, the improved $\gamma - Re_\theta$ two-equation turbulence model as well as the UDF function of Fluent are both adopted to control the experimental correlation formula in the transition model and better solutions of this problem are achieved.

Based on Menter's SST model, Langtry and Menter[4-6] put forward the $\gamma - Re_\theta$ model which could associate the transition starting point and the length of transition zone. Two transport equations about transition intermittent factor and transition initiation thickness Reynolds number were introduced.

(1) Intermittent factor transport equation:

$$\frac{\partial(\rho\gamma)}{\partial t} + \frac{\partial(\rho U_j \gamma)}{\partial x_j} = P_\gamma - E_\gamma + \frac{\partial}{\partial x_j} \left[\left(\mu + \frac{\mu_t}{\sigma_f} \right) \frac{\partial \gamma}{\partial x_j} \right] \quad (1)$$

(2) Transition initiation thickness Reynolds number transport equation:

$$\frac{\partial(\rho \bar{Re}_{\theta t})}{\partial t} + \frac{\partial(\rho U_j \bar{Re}_{\theta t})}{\partial x_j} = P_{\theta t} + \frac{\partial}{\partial x_j} \left[\sigma_{\theta t} (\mu + \mu_t) \frac{\partial \bar{Re}_{\theta t}}{\partial x_j} \right] \quad (2)$$

Among the source terms of the transition, $Re_{\theta c} = f(\bar{Re}_{\theta t})$ is used to associate with the starting point and

$F_{length} = f(\bar{Re}_{\theta t})$ is used to associate with the transition length. Re_α is the transition initial Reynolds number and is given by experiment relation formula in Fluent solver. $F_{\theta t}$ is blending function to turn off the boundary layer source term and the control of transport options of $\bar{Re}_{\theta t}$.

The solution is firstly performed with conventional $\gamma - Re_\theta$ turbulence model and the initial data of flow field are obtained for the following PSE solution. Then the gained outer boundary layer parameters are passed to the PSE solver for boundary layer flow stability analysis. In this step, the most critical issue is to use the location of the starting instability point and the transition point gained from boundary layer analysis to modify the critical transition Reynolds number $Re_{\theta c}$ and the initial transition Reynolds number $Re_{\theta t}$ based on the formulate(3)-(6) in reference[13]. This step is used to replace the experience coefficients of Fluent transition model to close the transition model. Finally, using UDF function, substituting the revised transition formula into the Fluent transition factor and momentum thickness Reynolds number of the transport equation, solving the flow field until it convergences as is shown in figure1.

$$Re_{\theta c} = \frac{\bar{Re}_{\theta t}}{(-0.042Tu_\infty^3 + 0.4233Tu_\infty^2 + 0.0118Tu_\infty + 1.0744)} \quad (3)$$

$$Re_{\theta t} = [1173.51 - 589.428Tu + \frac{0.2196}{Tu^2}] \cdot F(\lambda_\theta), Tu \leq 1.3.$$

$$Re_{\theta t} = 331.5 \cdot [Tu - 0.5658]^{-0.671} \cdot F(\lambda_\theta), Tu > 1.3. \quad (4)$$

$$F(\lambda_\theta) = 1 - [-12.986\lambda_\theta - 123.66\lambda_\theta^2 - 405.689\lambda_\theta^3] \cdot e^{-\frac{Tu}{0.5}}, \lambda_\theta > 0. \quad (5)$$

$$Tu = 100 \frac{\sqrt{2k/3}}{U}, \lambda_\theta = \frac{\rho\theta^2}{\mu} \frac{dU}{ds}. \quad (6)$$

Which are illustrated in detail in reference[13]. While coupled with Fluent, a code for UDF is compiled in the following form:

```
#include "udf.h"
DEFINE_TRANS_FLENGTH(user_Flength, c, t)
{
    ...//
}

DEFINE_TRANS_RETHETA_C(user_Re_thetac, c, t)
{
    ...//
}

DEFINE_TRANS_RETHETA_T(user_Re_thetat, c, t)
{
    ...//
}
```

Reference [13] used these relation equations to solve $Re_{\theta c}$ and F_{length} in order to close transition model equations.

However in this paper, PSE boundary layer stability analysis method is applied to deal with them.

III. PSE STABILITY EQUATIONS^[15]

Before applying the nonlinear boundary layer stability analysis to the methodology developed in this paper, the open forms of Linear Stability Theory (LST) and Parabolized Stability Equation (PSE) are introduced firstly. To derive the LST, the flow is assumed to be locally parallel. Substituting the disturbance quantities into the linearized Navier Stokes equations, it can be obtained the first order differential equations of LST in matrix form:

$$q'(x_1, x_2, x_3, t) = \hat{q} e^{i(ax_1 + \beta x_3 + \omega t)} \quad (7)$$

$$\frac{d\hat{q}}{dx_2} = A_0 \hat{q} \quad (8)$$

$$\hat{q} = [\hat{u}_1, \frac{d\hat{u}_1}{dx_2}, \hat{u}_2, \frac{d\hat{u}_2}{dx_2}, \hat{T}, \frac{d\hat{T}}{dx_2}, \hat{u}_3, \hat{p}]^T \quad (9)$$

In general the three dimensional boundary layer are not parallel, substituting the disturbance forms into the linearized Navier-Stokes equations, it can be obtained the second order differential equations of PSE written in matrix form:

$$q'(x_1, x_2, x_3, t) = \hat{q}(x_1, x_2) e^{i(a(x_1)x_1 + \beta x_3 + \omega t)} \quad (10)$$

$$A_1 \frac{\partial^2 \hat{q}}{\partial x_1^2} + A_2 \frac{\partial^2 \hat{q}}{\partial x_2^2} + B_1 \frac{\partial^2 \hat{q}}{\partial x_1 x_2} + C_1 \frac{\partial \hat{q}}{\partial x_1} + C_2 \frac{\partial \hat{q}}{\partial x_2} + D_1 \hat{q} = 0 \quad (11)$$

$$\hat{q} = [\hat{p}, \hat{u}_1, \hat{u}_2, \hat{u}_3, \hat{T}]^T \quad (12)$$

Then the nonlinear PSE equations are developed based on the assumption of small perturbation as illustrated in this paper. Nonlinear PSE equations are based on the assumption of small perturbation and can be directly used to solve three-dimensional problems. The fluctuations of pressure, density, temperature, viscosity, thermal conductivity and other physical quantities are taken into account in calculation[7].

In this paper, the disturbance variation in curved coordinate is adopted as follows:

$$q' = \tilde{q}(s, n) \exp\left(i\left[\int_{s_0}^s \alpha(s) ds + \beta \cdot z + \omega \cdot t\right]\right) \quad (13)$$

In which, $q' = [\rho', u', v', w', T']^T$ is the disturbance quantity. α and β are respectively the wave number of flow direction and radial direction. ω is the disturbance frequency and s is the curve coordinate along flow direction. $\tilde{q}(s, n)$ is the disturbance amplitude. This perturbation is substituted into the Navier Stokes equations and the mean flow is subtracted, then the nonlinear disturbance equation in orthogonal curvilinear coordinates is as follows:

$$\frac{\partial q'}{\partial t} + \mathbf{V}_s \frac{\partial q'}{\partial s} + \mathbf{V}_n \frac{\partial q'}{\partial n} + \mathbf{V}_r \frac{\partial q'}{\partial r} + Vq' = \mathbf{V}_{ss} \frac{\partial^2 q'}{\partial s^2} + \mathbf{V}_{nn} \frac{\partial^2 q'}{\partial n^2} + \mathbf{V}_{rr} \frac{\partial^2 q'}{\partial r^2} + \mathbf{V}_{sn} \frac{\partial^2 q'}{\partial s \partial n} + \mathbf{V}_{sr} \frac{\partial^2 q'}{\partial s \partial r} + \mathbf{V}_{nr} \frac{\partial^2 q'}{\partial n \partial r} \quad (14)$$

In which V , V_i and V_{ij} are all 5×5 operator matrixes.

Based on the assumptions that the disturbances are composed of a fast-oscillatory wave part and a slowly-varying shape function, the disturbance equation above is simplified into the following form:

$$\left(A_2 \frac{d^2}{dn^2} + A_1 \frac{d}{dn} + A_0\right) \phi = \frac{B}{\text{Re}} \frac{\partial \phi}{\partial x_s} - \frac{\mathbf{V}_{ss}}{\text{Re}} \frac{\partial \phi}{\partial x_s} - \frac{\mathbf{V}_{sn}}{\text{Re}} \frac{d^2 \phi}{dx_s dn} \quad (15)$$

This is an eigenvalue problem and can be solved through numerical discretization method. The boundary conditions are as follows:

$$\tilde{u} = \tilde{v} = \tilde{w} = \tilde{T} = 0, \quad y = 0; \quad (16)$$

$$\tilde{u} = \tilde{v} = \tilde{w} = \tilde{T} = 0, \quad y \rightarrow \infty. \quad (17)$$

Since the disturbance evolutions are mainly focused on the stream-wise and normal direction for specific problems, the PSE analysis system above is also suitable for prediction of two-dimensional or axi-symmetric flows. For the 2D and axi-symmetric flow models discussed in the following, a finite thickness is assumed in the cross (or the span-wise) direction, in which the disturbance quantity is set to be 0 during the 3D solver marching process.

In order to accurately solve the boundary layer equations, sufficient number of grid points is needed within the boundary layer calculation region. In this paper, 200-300 points can be arranged in the normal direction of the wall and high-precision spectroscopy method is used to solve the discrete boundary layer disturbance equations. During the solving process of the nonlinear PSE equations, the solution variables $\alpha(\xi)$ and $\Phi(\xi, \eta)$ needs to be updated.

$$\alpha^{new} = \alpha^{old} - \frac{i}{E} \int_{\Omega} \bar{\rho}(u^{*+} \frac{\partial u'}{\partial \xi} + v^{*+} \frac{\partial v'}{\partial \xi} + w^{*+} \frac{\partial w'}{\partial \xi}) dn \quad (18)$$

The introduction of energy conservation condition on the above equation can eliminate the correlation of n :

$$E = \int_{\Omega} \bar{\rho}(|u'|^2 + |v'|^2 + |w'|^2) dn \quad (19)$$

The superscript "+" in the equation indicates complex conjugate. So the transition prediction can be done by accumulating disturbance growth rate along flow direction. Its integral form is as follows:

$$N(\omega, s) = \int_{s_0}^s \left[-\text{Im}(\alpha) + \frac{1}{2E} \frac{dE}{ds}\right] ds \quad (20)$$

In which, s_0 is the first position of a neutral point within a given frequency. In this way, the occurrence of transition can be predicted by the size of N values.

A detailed derivation of the above equations and the validation of PSE calculation process can be seen in Reference [15].

IV. RESULTS AND DISCUSSION

A. SE Application

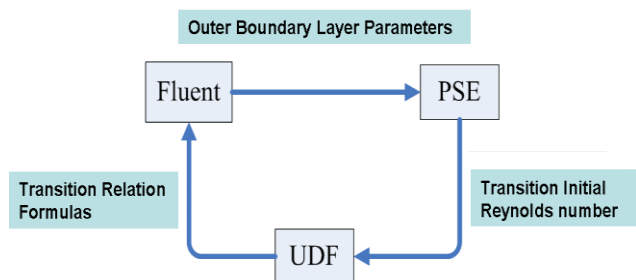


Fig.1. Schematic diagram of the solution process

In this paper, the solution schedule mainly includes the following three steps. First, the model is preliminary calculated using Fluent software and the transition models (for example the $\gamma - Re_\theta$ model) using conventional common empirical coefficient. Then, the gained outer boundary layer parameters are passed to the PSE solver for boundary layer flow stability analysis. In this step, the most critical issue is to use the location of the starting instability point and the transition point gained from boundary layer analysis to modify the critical transition Reynolds number $Re_{\theta c}$ and transition initial Reynolds number $Re_{\theta t}$ based on the formulate(3)-(5) in reference[13]. This step is used to replace the experience coefficients of Fluent transition model to close the transition model. Finally, using UDF function, substituting the the revised transition formula into the Fluent transition factor and momentum thickness Reynolds number of the transport equation, solving the flow field until it convergences. Fig.1 illustrate the solving process.

The grid sensitivity for the numerical simulation of transitional boundary layer has been studied in detail[14,15], which point out that the Menter & Langtry(SST Gama) turbulence model has better ability to the simulation of boundary layer transition. Through the specification of transitional onset momentum Reynolds number and inlet viscosity ratio from test data or designer experience, it is able to provide better simulation of heat transfer within transitional boundary layer. Specially the SST model has higher requirement for the numerical grid density with the first layer grid nodes near wall surface satisfying $y^+ < 1$. In this paper all cases are computed on the grid with $0.05 < y^+ < 0.5$ for the first grid layer near the wall surface. While for the grid sensitivity for the PSE solver, it is performed during the TS wave stability analysis for the specified simulation, where

only the absolutely similar wave numbers obtained on two different grids are considered to be confidential.

The current studies[2] have shown that when the incoming flow Mach number is less than 4, the flow instability of the focus mode is a first-order mode (TS mode). When the Mach number is greater than 4, the master transition process is the second-order mode disturbance. For the cone hypersonic flow model, due to a relatively low velocity after bow shock, it is difficult to find the instability second-order mode. Therefore, to study the instability of boundary layer flows, this paper introduce the PSE equations to calculate the first-order mode wave (TS wave) while the initial disturbance frequency is 200khz. For the application of TS wave to the transitional hypersonic flow in this paper, it is attempted to predict the most unstable location of the boundary layer, the precise disturbance amplification rate maybe not necessary. Only the approximate unstable locations should be specified to provide the key transitional parameters such as the critical transition Reynolds number $Re_{\theta c}$ and the initial Reynolds number $Re_{\theta t}$, which are needed to complete the coupling solution with mean flow code. So only TS wave(the 1st mode) is considered for simplification and the conclusion is validated.

B. Case 1[16]

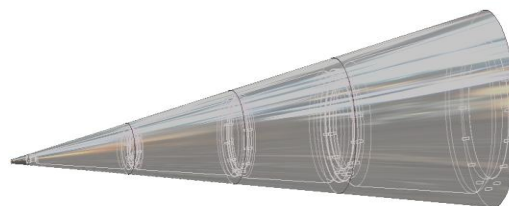


Fig.2. Geometry Model of a Cone

Initial mean flow solution

Fig.2 is the geometry model of a cone, The cone angel of the model is 7 degree, cone length is 2.35m and the head radius is 5mm. The inflow Mach number M_∞ is 7.15, inlet pressure P_∞ is 7722Pa and inlet temperature T_∞ is 214K. The temperature at cone wall T_w is 300K. Two-dimensional axisymmetric calculation method is applied. y^+ is less than 0.5 and Tu_∞ is about 0.01%.

The solution is firstly performed with conventional $\gamma - Re_\theta$ turbulence model and the initial data of flow field are obtained for the following PSE solution.

Eigen-value solution on two sets of grid configurations

Fig3 displays the real and imaginary part of stream-wise wave number α at different axial positions of 0.2 and 0.85. As is shown in the figure that the eigenvalue solution is performed on two sets of grid configurations, with the grid nodes 300×151 and 300×251 respectively. Let n_x represents the grid node number in streamwise direction(parallel to the wall), and n_y in normal direction(perpendicularly to the wall). It is considered in this paper that the same eigenvalue solved under normal grid nodes of $n_y=151$ and $n_y=251$ is reasonable for PSE solution, and the eigenvalue with the minimum

imaginary part represents for the one which leads to the most instability of the flow.

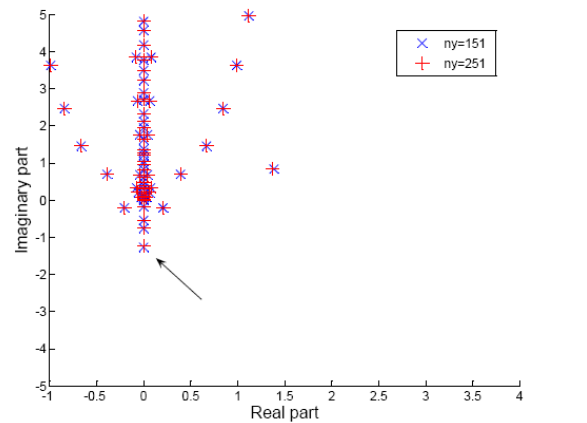
The current studies[2] have shown that when the incoming flow Mach number is less than 4, the flow instability of the focus mode is a first-order mode (TS mode). When the Mach number is greater than 4, the master transition process is the second-order mode disturbance. For the cone hypersonic flow model, due to a relatively low velocity after bow shock, it is difficult to find the instability second-order mode. Therefore, to study the instability of boundary layer flows, this paper introduce the PSE equations to calculate the first-order mode wave (TS wave) while the initial disturbance frequency is 200khz. For the application of TS wave to the transitional hypersonic flow in this paper, it is attempted to predict the most unstable location of the boundary layer, the precise disturbance amplification rate maybe not necessary. Only the approximate unstable locations should be specified to provide the key transitional parameters such as the critical transition Reynolds number $Re_{\theta c}$ and initial Reynolds number $Re_{\theta t}$, which is needed to complete the coupling solution with mean flow code. So only TS wave(the 1st mode) is considered for simplification and the conclusion is validated.

Mean flow solution coupled with PSE analysis results

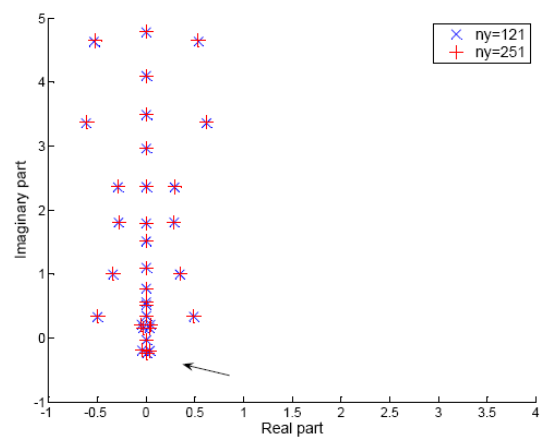
Fig.4(a) shows the wave-number distribution along flow direction. The starting location of the instability point is located at $x=0.35$, the location of the most unstable point is at $x=0.65$ where the N value is 7.2 here, as is shown in Fig.4(b). According to the formula (3) the calculation the critical transition Reynolds number $Re_{\theta c}$ and initial Reynolds number $Re_{\theta t}$ on these two positions is carried out and finally determines F_{length} . So that these three parameters can be re-substituted into transport equations, through the UDF compile processed, continue to iteratively solve the whole flow field. The wall heat flux distribution is shown in Fig.5. As we can see, there is a serious deficiency in transition simulation process while applying traditional method. If transition model is used directly, the length of the transition zone, as well as the wall heat flux of the transition process have been predicted a larger deviation. The transition zone is too small and the heat flow is significantly high. The empirical parameters of the transition model need to be constantly adjusted. When using this transition amendment method of this article, because it can more accurately give the starting transition Reynolds number, the occurrence and development of the transition process simulated are more rationalized. The lengths of the transition zone and heat flux after transition are more close to experimental results. This is very useful to simulate a complex simulation of hypersonic wave structures, separation of boundary layer flows and aerodynamic heating phenomena.

It should be pointed out that the value of N used in this article only was an accurately one as long as possible. That is said, if the obtained transition momentum thickness Reynolds number is more accurate, the calculation of the transition process can be improved. This greatly reduces the designers'

dependence on empirical parameters. Currently one of the problems is the PSE analysis process requires a different density level of the grid, through the shooting method to derive characteristic matrix eigenvalues, to find the minimum and the imaginary part of eigenvalues at different grids overlap levels as an expression of flow field in the most unstable point. Thus, when the grid point increase n times, the matrix size will be $n \times n$ times and the computing time will also increase $n \times n$ times. The PSE actual time-consuming of this article roughly is equivalent to a flow field calculation time. How to improve the speed of PSE solution will be discussed in the next step.



(a) $s=0.2$



(b) $s=0.85$

Fig.3. The real and imaginary part of stream-wise wave number a at different axial positions(a) $s=0.2$, (b) $s=0.85$

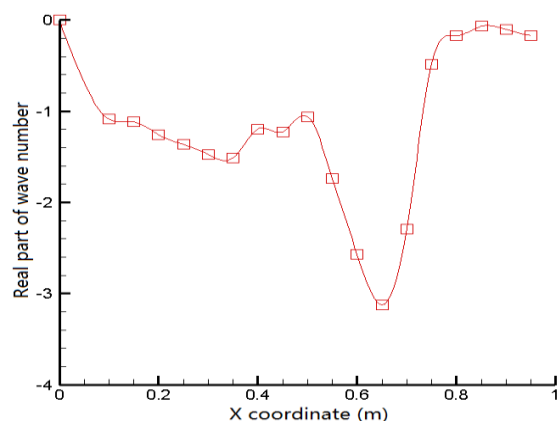


Fig.4 . Distribution of stability analysis factors on Cone Surface (a)Wave Number

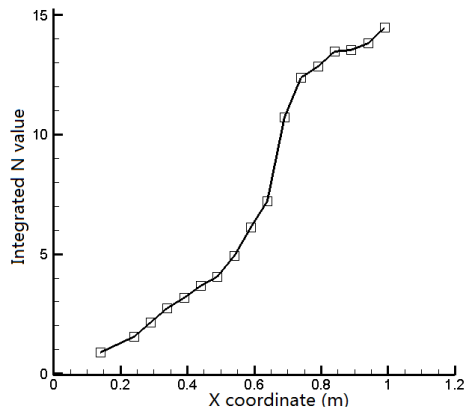


Fig.4. Distribution of stability analysis factors on Cone Surface, (b) Integrated N Vales

c. Case 2^[17]

Fig.6 is the numerical calculation model. The supersonic flow passes through an inclined board, creates a shock wave by compression effect. The shock incidents to the plate boundary layer and thus leads to a shock wave/boundary layer interference. The ramp length is $8.89 \times 10^{-2}m$ and the flat length is $30.48 \times 10^{-2}m$. The plane angel α and leading edge coordinate C are shown in Table.1. The inlet conditions are as follows:

$Re_L = 1.5 \times 10^5$, $M_{\infty} = 2.96$, $Tu_{\infty} = 0.2\%$,
 $T^* = 247K$ and $p^* = 4.07 \times 10^5$. All the walls are treated as adiabatic. The grid nodes for mean flow calculation are 200×200 , and $y^+ < 1$.

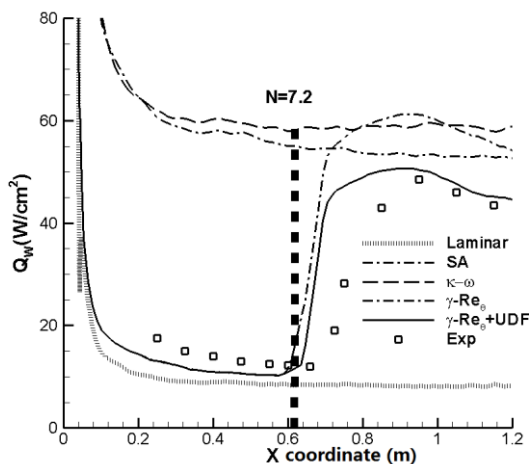


Fig.5. Heat Flux Rate on Cone Surface

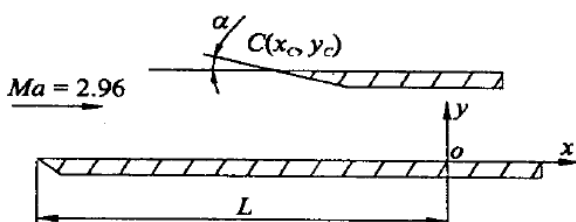


Fig.6. Numerical Calculation Model

Table1. Plane Angel α and Leading Edge Coordinate

(x_c, y_c)		
$\alpha / (^\circ)$	$x_c / 10^{-2}m$	$y_c / 10^{-2}m$
9.39	-9.144	4.674
12.27	-9.500	5.436

As is shown in Fig.7 the wall pressure numerical results are compared with the experimental values. The pressure suddenly rises through the shock wave. After the shock wave, the subsonic flow passes back through the boundary layer against the mainstream so that the pressure upper of the shock incident wave rise. So boundary layer separation occurs before the shock incident point. At this situation, $\gamma-Re_\theta$ transition model of Fluent Software is used to accurately obtain the value of pressure increase after shock wave. However, the location of separation point and re-attach point and the length of separation zone are still having a certain degree of deviation. Especially for the situation when α equals 12.27degree, the predicted separation zone is a little lager and the separation point is obviously moved upwards. By using the methods above, the boundary layer stability analysis is carried out while N is selected as 8.0. The initial Reynolds number at the boundary layer instability transition point is gained. Applying the revised $\gamma-Re_\theta$ transition model, an accurate pressure rise is obtained ($\alpha = 9.39$, $p/p_0 = 3.85$ while $\alpha = 12.27$, $p/p_0 = 4.9$). The prediction of the location of separation point and re-attach point and the length of separation zone has a good fit with the experimental values. In particular, the location of the pressure sudden increase, the pressure of the pressure platform area and the subsequent pressure stable value are well agreed with experiments. It indicates that the solution of this article is better than those using traditional turbulence model. See from Fig.8 and Fig.9, the calculation method of this paper accurately calculates the shock wave structure that contains shock incident to the laminar boundary layer on a plate after the shock wave reflection, expansion, and re-compression. The calculation is in good agreement with the experimental results.

Figure 10 shows the distribution of the axial component u along the normal direction of the wall, in which x1 and x7 denote the section surface outside of the separation region, x2 and x6 represent section surfaces passing through the separation and reattachment points, and x3, x4 and x5 stand for the sections within separation region. From the figure it can be seen the significant influence of the shock wave on the velocity distribution of boundary layer.

D. Case 3^[18]

Hypersonic axial symmetric compression corner flow with a skirt section is a typical example to verify the CFD

prediction capacity of hypersonic flow surface pressure and heat flux. The inlet flow conditions are: $T_w = 311K$, $M_\infty = 7.05$, $p_\infty = 576.0pa$ and $T_\infty = 81.2K$. The skew angle of the skirt section is 35 degree. The thickness of boundary layer is 2cm before the corner separation point. Two-dimensional axial symmetric calculation is adopted.

The grid nodes are 200×200 and $y^+ < 0.5$.

Fig.11 is a typical geometry model of corner compression in hypersonic flow. N is selected as 8.0 when calculating boundary layer stability by PSE method. Joint with flow field solution, wall pressure has been shown in Fig.12 and wall heat flux density shown in Fig.13. In these figures, the results are compared with the experimental values and those do not use PSE for transition model updating. By comparison you can see, the application of PSE on amendment of transition gets a more accurate pressure distribution and heat flow rate peak, especially for the peak position forecast. At the same time, the heat flow overshoot phenomenon right after the peak pressure is described more clearly. It has obvious advantages in comparison with no amendments to the transition model. This is very meaningful to the heat protection design of hypersonic aircrafts.

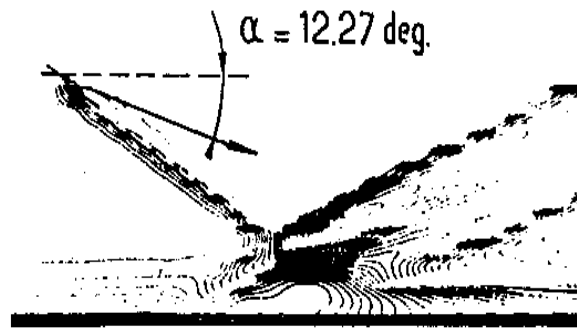


Fig.8. Contours of Density in Interaction Zone (Exp) [9]

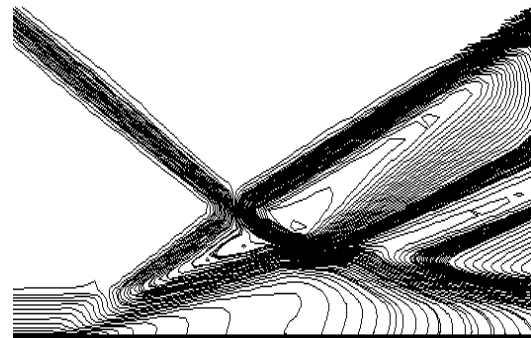


Fig.9. Counters of Density in Interaction Zone (Numerical)

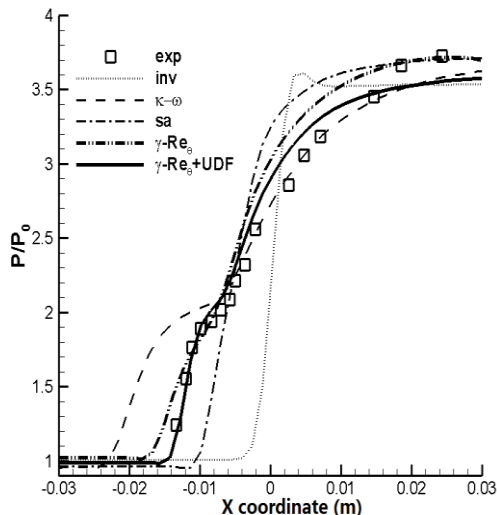


Fig.7. Pressure distribution on Flat Surface (a) $\alpha = 9.39^\circ$

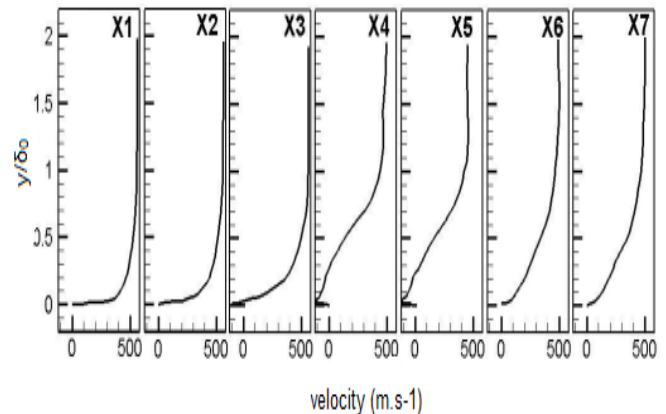


Fig. 10. Distribution of axial velocity in the interaction zone

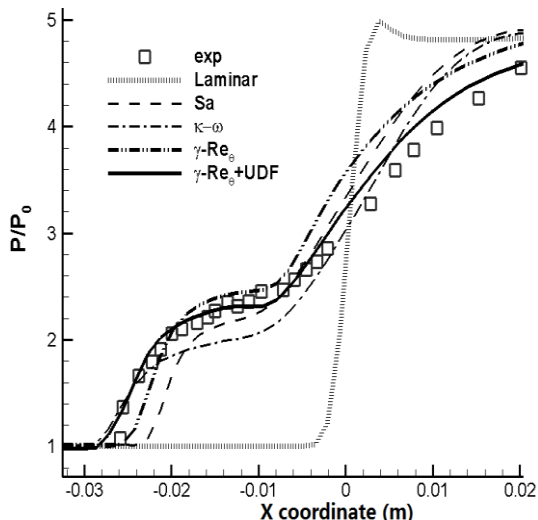


Fig.7. Pressure distribution on Flat Surface (b) $\alpha = 12.27^\circ$

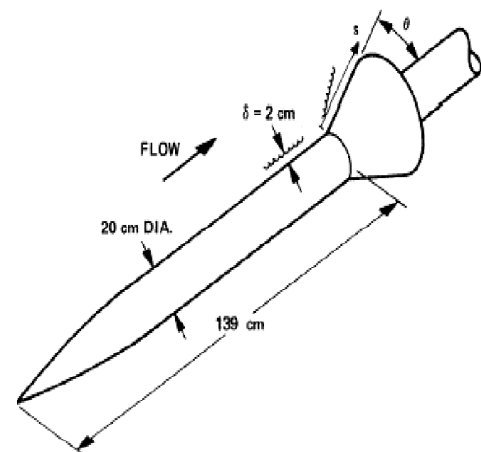


Fig.11. Geometry Model of Corner Compression in Hypersonic Flow

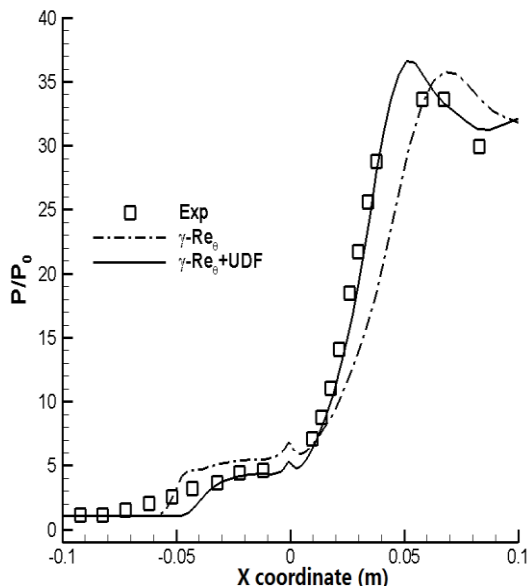


Fig.12. Wall Pressure

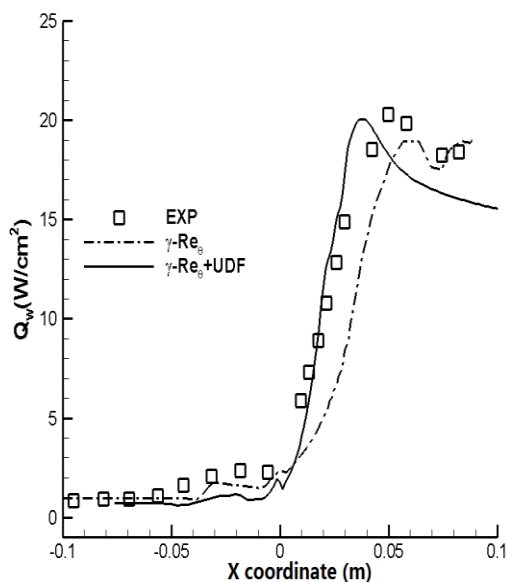


Fig.13. Wall Heat Flux Rate

Fig.14 shows the density and pressure isolines within the interaction region, in which a represents a weaker shock wave caused by the concave of the stream lines near the separation point of the boundary layer. b is a strong shock wave from the reattachment point in separation region, which interacts with shock a, forming a stronger shock wave c. The flow behind shock wave b comes from the free incoming flow only compressed by shock wave c, so the flow energy loss behind shock wave b is not large, with higher local pressure there. Therefore a set of expanding waves are created, leading the pressures behind shock wave b and c to be equilibrium. The above illustration of wave structure can be verified through the comparison with reference[19]. In the fig.15 of the pressure isolines, it is shown that a higher pressure region exists behind the reattachment point, which is corresponded to the wall pressure overshoot. The reattachment point is at $x=0.025\text{m}$ and the pressure overshoot is at $x=0.035$, the two positions are very close.

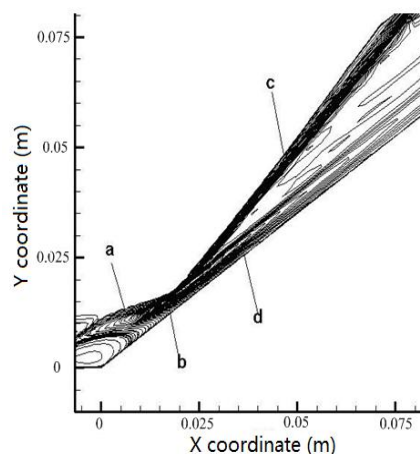


Fig.14. Density distribution in interaction zone

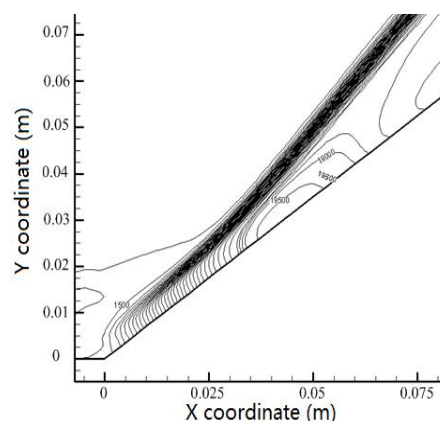


Fig.15. Pressure distribution in interaction zone

V. CONCLUSIONS

Following the hypersonic flow transition phenomenon, the PSE disturbance equations and N-S equations have been solved jointly and semi-empirical e^N method has been employed in the present numerical investigation. The objective is to identify the unstable point within the boundary layer so that the $\gamma-Re_0$ turbulence model could be amended in Fluent software, correlating the transition relation formulas with Reynolds number based on initial momentum thickness, the critical Reynolds number as well as the transition zone length. It successfully reduced the reliance upon the experiments and experiences during the transition region in the hypersonic flow process. For the complex transition flow around cone surface within the hypersonic flow regime, and the interaction between shock wave and boundary layer, the capability of $\gamma-Re_0$ turbulence model and associated guidelines have been proven yielding to more accurate supersonic and hypersonic numerical results.

NOMENCLATURE

- T : Temperature(K)
- λ : Thermal conductivity(W/mK)
- ρ : Density(Kg/m³)
- p : Pressure(Pa)
- h : Convective heat transfer coefficient(W/m²K)
- U : Flow quantities

q, ω : Turbulence quantities
 \tilde{U} : Disturbance Amplitude
 \bar{U} : Mean flow quantities
 s : Stream-wise direction
 U' : Disturbance quantities
 n : Normal direction
 α : Stream-wise wave number
 β : Span-wise wave number
 f : Disturbance frequency
 t : time(s)
 A_0, A_1, A_2 : Matrix
 i : Imaginary part
 Tu_∞ : incoming turbulence intensity
 Tu : local turbulence intensity
 γ : Intermittent factor
 \bar{Re}_{θ_t} : transported momentum thickness Reynolds number
 Re_{θ_t} : initial transition Reynolds number
 Re_{θ_c} : critical transition Reynolds number

- [13] Krause M, Behr M, Ballmann J. Modeling of transition effects in hypersonic intake flows using a correlation-based intermittency model [R]. AIAA paper, 2008-2598.
 [14] Dong Ping. Research on Conjugate Heat Transfer simulation of Aero Turbine Engine Air-cooled Vane[D]. Dissertation for PH.D. Harbin Institute of Technology, Harbin,2009.
 [15] Dong xuezhi. Application Research of PSE Approach in Flow Stability Prediction on Blade Surface[D]. Dissertation for PH.D. Harbin Institute of Technology. 2007.
 [16] Maclean M, Mundy E, Johnson H. Comparisons of transition prediction using PSE-Chem to measurements for a shock tunnel environment [R]. AIAA paper, 2007-4490.
 [17] Lei Yubing , Lang Dew ang , Huang Guop ing. Numerical Study of Shock Wave Turbulent Boundary Layer interaction in Supersonic Flows[J]. Journal of Nan jing University of Aeronautics &Astronautics. 2004 · 36(1) : 1-5.
 [18] He, xuzhao. Numerically Simulate Aero-Force&Heat of Hypersonic Vehicles and Region Marching Method of Supersonic Flow Simulation [D]. Dissertation for PH.D. China Aerodynamics Research and Development Center, 2007.
 [19] Elfstrom G M. Turbulent Hypersonic Flow at a Wedge Compression Corner[J]. Journal of Fluid Mechanics. 1972, 53(1):113-127.

ACKNOWLEDGMENT

The project is sponsored by National Nature Science Foundation (50706009).

REFERENCES

- [1] Dong Ming , Zhou Heng. Examination of the application of BL model in supersonic turbulent boundary layers [J]. Acta Aerodynamic Sinica, 2009 · 27(1) : 102-107.
 [2] Papp J L, Dash S M. A rapid engineering approach to modeling hypersonic laminar to turbulent transitional flows for 2D and 3D geometries [R]. AIAA paper. 2008-2600. 2008.
 [3] Helen L R, Eduardo P, and Joseph K. Hypersonic stability and transition Prediction[R]. 21st AIAA Computational Fluid Dynamics Conference. AIAA paper. 2013-2556. 2013.
 [4] F. R Menter. Two-Equation Eddy-Viscosity Turbulence Models for Engineering Applications[J][AIAA Journal, 1994, 32(8):1598~1605.
 [5] Langtry, R. A correlation-based Transition Model using Local Variables for Unstructured Parallize CFG Codes[D]. PH.D Thesis, Stuttgart University, 2006, 37-56.
 [6] Menter, F. and Langtry, R. A Correlation-Based Transitional Model Using Local Variables PartI – Model Formulation[J]. Proceeding of ASME Turbo Expo. 2004.
 [7] Th. Andre. and I. Fedioun THypersonic Boundary-Layer Transition Tripped by Wall Injection: Global Mode Analysis[R]. 20th AIAA International Space Planes and Hypersonic Systems and Technologies Conference. AIAA 2015-3525. 2015.
 [8] Johnson, H. and Candler,G. Hypersonic Boundary Layer Stability Analysis Using PSE-Chem[R]. 35th AIAA Fluid Dynamic Conference and Exhibit, AIAA Paper 2005-5023,2005.
 [9] Yang Yunjun, Ma Handong, Zhou Chuangjiang. Numerical Research on Supersonic Flow Transition[J]. Journal of Astronautics. 2006 · 27(1) : 85-88.
 [10] Cai Qiaoyan; Tan Huijun. Effects of the fore-body boundary layer state on flow structure and performance of hypersonic inlet[J]. Journal of Aerospace Power. 2008,23(4):699-705.
 [11] Dong Hao; Wang Chengpeng; Chen Keming. Investigation of flow characteristic and performance on the "Jaws" hypersonic inlet[J]. Journal of Aerospace Power. 2009,24(11):2429-2435.
 [12]Roy CJ, Blottner F G. Assessment of one- and two-equation turbulence model for hypersonic transitional flows [J] Journal of Spacecraft and Rockets, 2001, 38 (5): 699-711.